Numerical Analysis of a Printed Dipole Antenna Integrated With a 3-D AMC Block

Aycan Erentok, *Member, IEEE*, Dongho Lee, and Richard W. Ziolkowski, *Fellow, IEEE*

***Abstract*—The integration of a printed electric dipole antenna into a volumetric metamaterial-based artificial magnetic conductor block is considered. It is demonstrated numerically that resonant modes can be excited to produce either large front-to-back ratios or large broadside directivities.**

***Index Terms*—Antennas, artificial magnetic conductor, metamaterials.**

I. Introduction

THE ultimate need to design application-specific antennas to satisfy the demanding environments of today's wireless communication systems and networks has been the focus of many researchers. A recent and popular approach is to use man-made artificially fabricated structures, so-called metamaterials, to improve certain physical and radiation characteristics of these antennas, e.g., reducing their size and improving their directivity etc. [1]. These metamaterials are artificial materials that have electromagnetic responses which are not generally found in nature. Well-known examples include frequency-selective surfaces (FSSs), electromagnetic bandgap (EBG) structures, and double negative (DNG) and single negative (SNG) media. A popular metamaterial application, due to its relative ease of fabrication, is to realize artificial magnetic conductors (AMCs), i.e., to fabricate a structure that produces in-phase reflections at a specified operating frequency and, hence, a reflection coefficient whose absolute value equals one and whose phase equals zero. This in-phase reflection property of AMCs has been of significant interest because of its potential as an enabling technology for low profile antenna designs.

This paper presents the physical integration of a transmission line (TL)-fed printed dipole antenna with the three-dimensional (3-D) AMC block introduced in [2]. We investigate two figures of merit. One is the significant improvement of the front-to-back ratio of the far-field radiation pattern, predicted in [2], which is associated with a resonant mode of the integrated structure. The other is the directivity of the integrated structure. The numerical analysis reveals that there is another mode of operation which causes the directivity of the printed dipole antenna to be improved by more than 200% when it is compared with the directivity value of the corresponding half-wavelength dipole.

Manuscript received September 15, 2006; revised February 4, 2007. This work was supported in part by DARPA Contract number HR0011-05-C-0068.

A. Erentok and R. W. Ziolkowski are with the Department of Electrical and Computer Engineering, University of Arizona, Tucson, AZ 85721-0104 USA.

D. Lee is with the Department of Electrical and Computer Engineering, University of Arizona, Tucson, AZ 85721-0104 USA and with LG Electronics, Mobile Handset R&D Center, Gumchon-gu, Seoul 153-801, Korea.

Color versions of one or more of the figures in this paper are available online at http://ieeexplore.ieee.org.

Digital Object Identifier 10.1109/LAWP.2007.893107

II. Analysis

The radiation characteristics of a printed dipole antenna fed by a rectangular TL in a sheet of Rogers 5880 Duroid was determined in the presence of a 3-D AMC block introduced in [2] for applications in the X-band near 10 GHz. This printed antenna design is integrated straightforwardly into the AMC block in one of its layers. The proposed 3-D AMC block can be constructed with only two unit layers of capacitively loaded loop (CLL) elements that are symmetrically positioned along the x-axis. The printed dipole is designed to be symmetric both in the x- and z-directions. The block layers are symmetric about the printed dipole layer in the x-direction. These symmetries enabled us to use symmetry planes in the Ansoft High Frequency Structure Simulator (HFSS) simulations to reduce significantly the overhead of the computations.

The unit layer of each CLL block consists of ten CLL elements in a 5×2 array in the yz-plane on a 31 mil sheet of Rogers 5880 Duroid TM ($\varepsilon_r = 2.2, \mu_r = 1$), with the middle two CLL elements being centered about the coordinate origin. The design specifications of each CLL element cell were summarized in [2]. Referring to Fig. 1, all of the line widths of the CLL elements were $\mathrm{T} = 18$ mil. The total y-length of each CLL was $\mathrm{L} = 100$ mil. The total z-length of each CLL was $\mathrm{W} = 160$ mil. The y-depth of the capacitive strips of each CLL was $\mathrm{S} = 49$ mil. The z-length of each segment of the split side of each CLL was $\mathrm{U} = 65$ mil. Thus, the capacitive gap size was 30 mil for each CLL. The x-length of each CLL was assumed to be infinitely thin and was treated in HFSS by applying perfectly electric conducting boundary conditions over each CLL surface. The G1 and G2 distances were 40 and 20 mil, respectively. The 3-D AMC block used here consists of ten CLL unit layers. The two center CLL elements were removed from both the fifth and the sixth unit layers to make room for the transmission lines that feed the printed dipole. Each CLL unit layer was aligned in the same direction with the gaps of the CLL elements facing towards the printed dipole to enhance the resonant high impedance behavior. The overall AMC block thus consists of 88 CLL elements and has xyz-dimensions $= 310 \times 260 \times 1000$ mil.

The printed dipole antenna was positioned along the y-axis, in front of the 3-D AMC block, to ensure that the principal plane of the antenna's magnetic field is along the xz-plane while its electric field principal plane is the yz-plane, the plane parallel to the CLL elements. This orientation provides the largest possible flux of the magnetic field through the CLL elements. As shown in [2], the distance h between the arms of the dipole antenna and the edge of AMC block can to be tuned to achieve a resonant antenna system. The substrates along the fifth and sixth

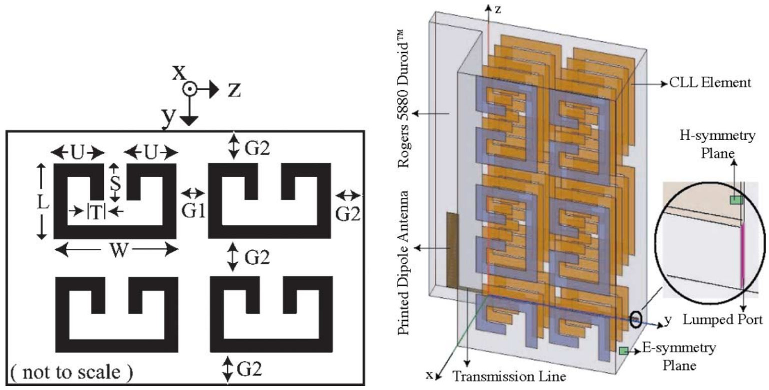

Fig. 1. Specifications of the two CLL element deep unit layer and the overall configuration showing the printed dipole antenna integrated into the 5 × 2 CLL unit layer-based AMC block.

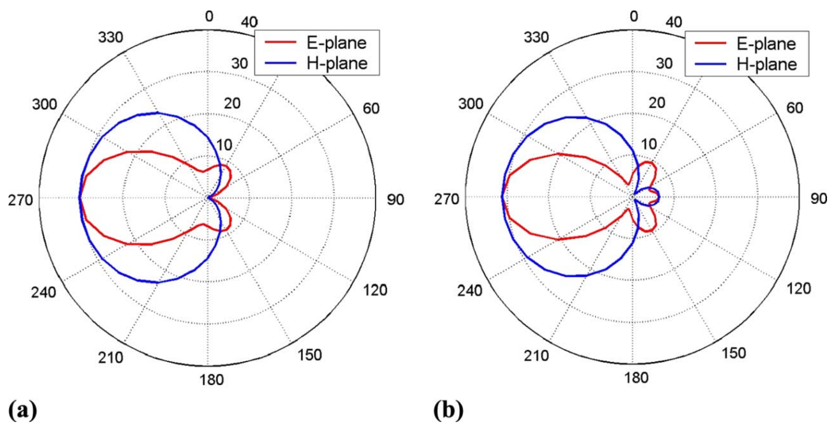

Fig. 2. The E- and H-plane radiation patterns of the (a) large front-to-back ratio and (b) large directivity resonant mode versions of the integrated printed dipole-AMC block.

unit cell layers were thus extended along the y-direction to provide the required tuning space. The distance along the y-axis between the inside edge of the printed dipole antenna and the outside edge of the AMC block was initially set to 18 mil, a distance value obtained from [3]. The distance h was then optimized using HFSS parametric studies. The widths of and the spacing between the two rectangular conductors of the TL lines were both set to 2 mil. The total TL length was set simply to 259 mil, 1 mil less than the AMC block's y-dimension plus h, which kept the conductors in the substrate and, hence, allowed the use of HFSS's lumped source to drive the transmission lines. The thickness of the dipole antenna and the rectangular conductors of the TL were set to 0.3 mil along the x-direction, e.g., 0.15 mil in the $\pm$ x-directions and centered at the origin, to allow the proper inclusion of the lumped element source into the transmission line feed in the HFSS model. The complex impedance value of the lumped element source was assigned as $Z_{\text{feed}} = 50\ \Omega$ or $Z_{\text{feed}} = 75\ \Omega$ depending on the design scenario. The 3-D AMC block formed with unit layers having ten CLL elements and the integrated TL-fed printed dipole antenna are shown in Fig. 1 in the presence of E- and H-symmetry planes.

The magnetic field interactions between the printed dipole antenna and the CLL elements exhibit different resonant behaviors as the antenna is positioned closer to or further away from the 3-D AMC block. The overall resonance behavior of the 3-D AMC block and the interaction of the CLL elements with the magnetic field also depend on the printed dipole antenna length and its width because these parameters affect the reactance behavior of the overall system. It was found that the dipole antenna length for a given frequency of operation must only be large enough to provide a sufficient amount of magnetic flux to cause the CLL elements in the AMC block to create the resonant mode. On the other hand, specific resonance behaviors strictly depend on the antenna size. It is possible to use small printed dipole antenna lengths ($\sim \lambda/10$) but then the efficiency of the antenna system is poor, e.g., the efficiency of a 94 mil ($\sim \lambda/13$) long antenna was found to be 20%. Similarly, it also is not desirable to use a very long antenna, e.g., one whose length is comparable to the half-length of the AMC block, because the AMC block provides an inductance value that is larger than the antenna's reactance value for all frequencies, thus causing an impedance mismatch which again makes the antenna system an inefficient radiator. The overall length of dipole antenna was set to 426 mil, approximately 40% of the overall height of the AMC block, to obtain the desired AMC behavior. The width of the antenna was set to 20 mil. The finite thickness of the dipole antenna provides an extra capacitance to the antenna system that shifts the resonant frequency location and also modifies the complex input impedance of the overall system.

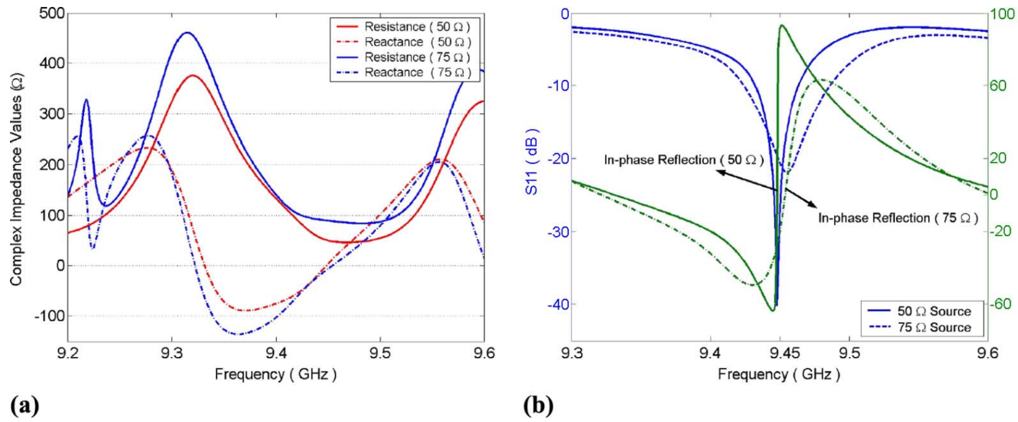

Fig. 3. The (a) complex impedance and (b) S_{11} magnitude and phase values for the large front-to-back ratio (50 Ω) and large directivity (75 Ω) resonant mode versions of the integrated printed dipole-AMC block.

TABLE I
SUMMARY OF THE PROPERTIES OF THE TWO RESONANT MODES OF OPERATION OF THE INTEGRATED PRINTED DIPOLE-AMC BLOCK

Resonant Frequency (GHz)	Directivity (dB)	S11 (dB)	TL spacing (mils)	Radiation Efficiency (%)	Front-to-Back Ratio (dB)
9.454	6.395	-21.8	2	89	44
9.448	7.033	-40.0	1.4	80	13.66

A parametric study was performed in which the distance between the antenna and the AMC block h was tuned to achieve a resonance. While the in-phase reflection property of the AMC block had been designed for 10 GHz, the introduction of the printed dipole shifts the resonance to lower frequencies. The optimal points were determined by observing the far-field radiation patterns of the overall antenna system. The HFSS simulations were run using E- and H-symmetry planes. The desired front-to-back ratio for the given integrated antenna-AMC block system was obtained using $h = 55$ mil and the corresponding resonance, an in-phase reflection point, was found at 9.454 GHz. Fig. 2(a) shows the far-field E- and H-field radiation patterns for this resonant frequency. Since the printed dipole is capacitive, the resonance frequency was lower than 10 GHz, the final design being dependent on the antenna parameters and the size of the AMC block. Fig. 3(a) and (b) shows the complex input and reflection behavior of this antenna system. The in-phase reflection point and minimum S_{11} value both occurred at the resonance frequency; which further confirms the high impedance behavior of the AMC block. The HFSS predicted front-to-back ratio was 160, i.e., 44 dB, in very good agreement with the value predicted with an idealized dipole configuration in [2]. Its directivity is 4.36 (6.395 dB), which is more than twice (2.58 times) the value of the same dipole radiating alone in free space. The HFSS simulations also demonstrated a different mode of operation for the same design for which the directivity is increased further, but at a cost of a poor S_{11} behavior and a reduced front-to-back ratio. The TL spacing for this design was then optimized to improve the S_{11} values of this alternate mode. This alternate mode of operation was also confirmed with different antenna-AMC block configurations. Fig. 2(b) shows the far-field radiation behavior of the same antenna design when the TL spacing was reduced from 2 to 1.4 mil at 9.448 GHz. Different from the first resonant behavior, the directivity of this modified structure at resonance improved 10% to 5.05 (7.033 dB) with a reduced front-to-back ratio, now only 4.8231 (13.66 dB). The complex input impedance and S_{11} values associated with this enhanced-directivity resonance are also shown in Fig. 3(a) and (b). Table I summarizes the radiation performance of these two different modes of operation of the integrated antenna-AMC block. The S_{11} values for the resonances at 9.454 and 9.448 GHz were obtained using $Z_{\text{feed}} = 75\ \Omega$ and $Z_{\text{feed}} = 50\ \Omega$, respectively. In contradistinction to the usual behavior of a resonant small capacitive dipole antenna, the antenna resonance occurs in both cases on the high-frequency side of the peak of the resistance curves. This is due to the dominant inductive behavior of the AMC block. Numerous simulation results, particularly in the presence of copper losses, have shown that it is easier and more practical to achieve the resonant mode that enhances the directivity of the printed dipole antenna than it is to find an efficient radiator that has a resonant mode that produces an extremely large front-to-back ratio.

III. CONCLUSIONS

A TL-fed printed dipole antenna was integrated into a 3-D AMC block and its design optimized numerically using HFSS. With one feed structure, it was resonant at 9.454 GHZ with a front-to-back ratio that was 44 dB and with a directivity of 6.395 dB. Another resonant mode of operation was also discovered for which the directivity of the antenna system was increased to 7.033 dB, but the front-to-back ratio was reduced to 13.66 dB.

REFERENCES

[1] N. Engheta and R. W. Ziolkowski, "A positive future for double negative metamaterials," *IEEE Microwave Theory Tech.*, vol. 53, pp. 1535–1556, Apr. 2005.

[2] A. Erentok, P. Luljak, and R. W. Ziolkowski, "Antenna performance near a volumetric metamaterial realization of an artificial magnetic conductor," *IEEE Trans. Antennas Propag.*, vol. 53, pp. 160–172, Jan. 2005.

[3] D. Lee, A. Erentok, and R. W. Ziolkowski, "Integration of a printed dipole antenna with a CLL-based volumetric metamaterial AMC block," in *2005 IEEE AP-S Int. Symp. USNC/URSI Nat. Radio Sci. Meeting*, Washington, DC, Jul. 3–8, 2005.